Structure-sensitive oxidation of the indium phosphide (001) surface

G. Chen, S. B. Visbeck, D. C. Law, and R. F. Hicks[a)]
Department of Chemical Engineering, University of California, Los Angeles, California 90095

(Received 15 November 2001; accepted for publication 1 March 2002)

The oxidation of anion- and cation-rich indium phosphide (001) has been investigated by exposure to unexcited molecular oxygen. Indium phosphide oxidation is an activated process and strongly structure sensitive. The In-rich $\delta(2\times4)$ surface reacts with oxygen at 300 K and above. Core level x-ray photoemission spectra have revealed that the O_2 dissociatively chemisorbs onto the $\delta(2\times4)$, inserting into the In–In dimer and In–P back bonds. By contrast, the P-rich (2×1) reconstruction does not absorb oxygen up to 5×10^5 Langmuir at 300 K, as judged by the unperturbed reflectance difference spectrum and low energy electron diffraction pattern. Above 455 K, oxygen reacts with the (2×1) inserting preferentially into the In–P back bonds and to a lesser extent into the phosphorus dimer bonds. © *2002 American Institute of Physics.*
[DOI: 10.1063/1.1471577]

I. INTRODUCTION

Compound semiconductors, such as gallium arsenide, indium phosphide, and their ternary and quaternary alloys, find extensive applications in high-speed integrated circuits and photonic devices.[1–7] A metal–oxide–semiconductor (MOS) technology for III–V materials has long been sought that would be as robust as the Si/SiO_2 system.[1,8–18] However, this has proven to be a difficult challenge, and nearly all commercial devices are based on heterojunctions or quantum wells that are grown epitaxially on top of a single crystal substrate. Although the oxides that form on these devices are not directly involved in their operation, they can still strongly affect performance.[9] For example, in heterojunction bipolar transistors, leakage currents across the oxidized surface tend to limit the amplifier gain.[19] Therefore it is important to better understand the nature of the oxide/compound semiconductor interface.

Indium phosphide has emerged as the only material that exhibits all the properties needed to implement the high-frequency components of 40 Gbit/s communications systems.[20] Both optical and electronic devices have been manufactured from indium phosphide and its alloys, including lasers,[21] modulators,[5] photodetectors,[22] and transimpedence amplifiers.[23] This makes InP the leading candidate for the development of optoelectronic integrated circuits (OEICs), and in particular, monolithically integrated 40 Gbit/s transceivers.[24]

Although the oxidation of indium phosphide has been studied in the past,[8–14] research on clean and ordered (001) surfaces is missing. The work published so far has examined the oxidation process after cleaning the substrate by wet chemical methods. This approach can yield a rough surface with numerous defects, and a residual oxide forms immediately upon rinsing the sample in deionized water. Moreover, the initial composition and structure of the surface prior to reaction is not well characterized in these studies. Uncertainties introduced by the chemical cleaning procedure have led to different conclusions regarding the mechanism of surface oxidation. Some authors have reported that In_2O_3 forms an inner layer and both indium and phosphorus atoms diffuse through this layer, forming $InPO_4$ at the surface.[25,26] Another research group has suggested that $InPO_4$ is generated below the surface, with indium out-diffusion to form In_2O_3 on top.[27,28] In this case, excess phosphorus accumulates at the oxide/semiconductor interface. Yet another group has proposed that P_2O_5 is formed during InP oxidation.[13]

To eliminate any artifacts introduced by sample cleaning methods, we have studied the oxidation of indium phosphide on clean and ordered (001) surfaces produced by metalorganic vapor-phase epitaxy. The two principal reconstructions formed on InP (001) are the phosphorus-rich (2×1) and indium-rich $\delta(2\times4)$.[29–35] Ball-and-stick models of these structures are presented in Fig. 1. The (2×1) is terminated by a complete monolayer of phosphorus dimers. Three valence electrons are distributed between two P dimer atoms (small dots in the picture). The P atom with the filled dangling bond is buckled up, while the other P atom with the half-filled dangling bond is buckled down. This model agrees well with scanning tunneling micrographs of this surface, which show zigzagging rows of gray spots extending along the [110] crystal axis.[29] The $\delta(2\times4)$ structure, with a phosphorus coverage of 0.125 ML, consists of a top layer In–P heterodimer sitting astraddle four second-layer indium dimers.[31,34] The indium dangling bonds are empty, while the phosphorus dangling bond is filled. Filled-states scanning tunneling micrographs of this surface show triangular shaped spots that form straight gray rows parallel to the $[\bar{1}10]$ direction.[31] The group of three spots are produced by the filled dangling bond of the P atom and the two In–In back bonds associated with the In–P heterodimer.[31,34]

In this article we report on the reaction of unexcited molecular oxygen with the (2×1) and $\delta(2\times4)$ surfaces of InP (001). Thin films of indium phosphide were deposited on single crystal substrates by metalorganic vapor-phase epitaxy

a)Author to whom correspondence should be addressed; electronic mail: rhicks@ucla.edu

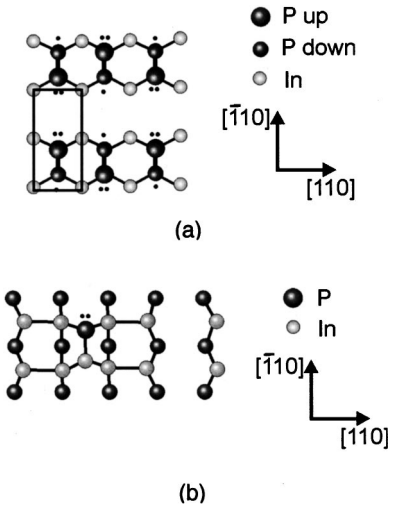

FIG. 1. Ball-and-stick models of the InP (001) surfaces: (a) (2×1) and (b) $\delta(2\times4)$ (see Refs. 25 and 27).

(MOVPE). Then the samples were transferred directly to ultrahigh vacuum, where the O_2 adsorption process was characterized by x-ray photoelectron spectroscopy (XPS), reflectance difference spectroscopy (RDS), and low energy electron diffraction (LEED). We have found that the oxidation rate strongly depends on the surface composition and proceeds by different mechanisms on the phosphorus-rich (2×1) and indium-rich $\delta(2\times4)$ reconstructions.

II. EXPERIMENTAL METHODS

Indium phosphide films, approximately 0.25 μm thick, were grown on *n*-type indium phosphide (001) substrates with a miscut of 0.75° towards the (111)*A* plane. The temperature during MOVPE was 835 K and the total reactor pressure was 20 Torr. Trimethylindium (TMIn) and tertiarybutylphosphine (TBP) were fed to the reactor at partial pressures of 5.5×10^{-4} and 0.1 Torr (V/III ratio of 180). After deposition, the TBP and hydrogen flows were maintained until the samples were cooled to 550 and 310 K, respectively. Then the InP crystals were transferred to a vacuum chamber with a base pressure of 3×10^{-10} Torr. Inside this system, the crystals were annealed to 625 and 720 K for 30 min to create the (2×1) and $\delta(2\times4)$ structures, respectively. Once the samples had cooled to 300 K, the reconstructions were confirmed by LEED.

Oxygen, ultrahigh purity grade (99.999%), was dosed onto the samples at pressures between 1.0 and 5.0 $\times10^{-5}$ Torr for different periods of time and at temperatures ranging from 300 to 720 K. All the filaments were turned off during exposure to avoid excitation or dissociation of the oxygen molecules. X-ray photoemission spectra were acquired before and after dosing at a take-off angle of 25° and a pass energy of 23.5 eV, using a PHI hemispherical analyzer with a multichannel detector and an Al$K\alpha$ source. Reflectance difference spectra were recorded on an Instruments SA J-Y NISEL reflectance difference spectrometer with baseline correction to remove any artifacts unrelated to the semiconductor surface states.[30]

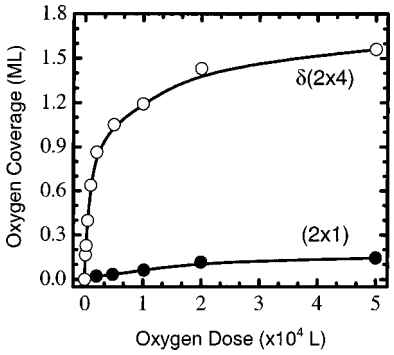

FIG. 2. Oxygen uptake on the (2×1) and $\delta(2\times4)$ structures as a function of O_2 exposure at 300 K.

The x-ray photoemission peaks were curve fitted using hybrid Gaussian–Lorentzian functions and a standard χ^2 minimization program. The thickness (d_{OX}) of the oxide overlayer present on the InP crystal was deduced from the peak intensities using the following equation:[36]

$$I_s = I_s^{\infty}\exp\left(-\frac{d_{OX}}{\lambda_{OX}\cdot\sin(\alpha)}\right), \tag{1}$$

where λ_{OX} is the photoelectron mean free path, equal to 26 Å,[37] and α is the take-off angle. The integrated peak intensities, I_S and I_S^{∞}, correspond to the surface with and without the oxide film. To ensure I_S was not unduly affected by the surface composition, the In $3d_{5/2}$ peak was used in the calculation for the P-rich (2×1), while the P $2p$ peak was used in the calculation for the In-rich $\delta(2\times4)$.

For the purposes of this study, it is more convenient to describe the oxygen adsorption in terms of the coverage, instead of the oxide thickness. This is particularly true when less than one monolayer is present on the surface. The oxygen coverage, θ, may be estimated by

$$\theta_{OX} = d_{OX}/t, \tag{2}$$

where t is the thickness corresponding to 1.0 monolayer (ML). This thickness is assumed to equal the height of one atomic layer in bulk indium phosphide, i.e., 1.5 Å.

III. RESULTS

Shown in Fig. 2 is the dependence of the oxygen coverage on the O_2 dosage at 300 K for the two different reconstructions. The curve for the $\delta(2\times4)$ exhibits a steep slope at the onset, followed by a gradual leveling off to 1.0 ML coverage at exposure greater than 1.0×10^4 Langmuir (1 L $=10^{-6}$ Torr·s). By contrast, the curve for the (2×1) rises much more slowly than the $\delta(2\times4)$, and it reaches a maximum value of only 0.2 ML at 5×10^5 L of O_2. The large difference in the initial slopes of the curves indicates that the indium-rich $\delta(2\times4)$ is much more reactive towards oxygen than the phosphorus-rich (2×1). It should be further noted that the (2×1) LEED pattern remains unchanged throughout the experiment, whereas the (2×4) LEED pattern transforms to (1×1) after dosing only 2000 L of O_2.

Presented in Fig. 3 are reflectance difference spectra of the (2×1) surface before and after exposure to 2.5×10^5 L

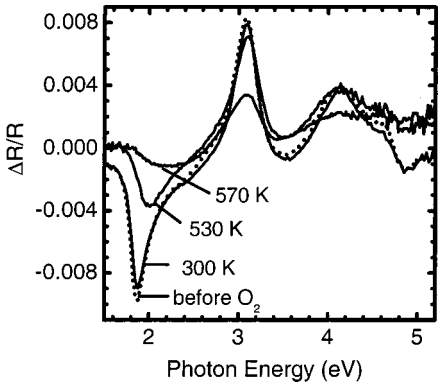

FIG. 3. Reflectance difference spectra of the (2×1) surface before and after oxidation at different temperatures.

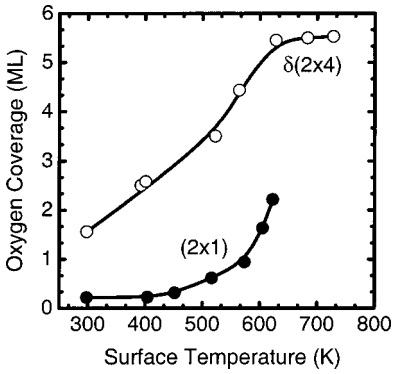

FIG. 5. Oxygen coverage as a function of temperature on the (2×1) and $\delta(2\times4)$ reconstructions at a dose of $(2.5 \text{ and } 1.8)\times10^5$ LO_2, respectively.

O_2 at different temperatures. The sharp positive peak at 3.1 eV is attributed to optical transitions involving surface phosphorus dimers. This feature, along with the intense negative peak at 1.8 eV, is considered to be the most sensitive to surface chemistry.[32,38,39] After dosing oxygen at 300 K, no significant change in the RD spectrum has occurred, indicating that the O_2 has not attacked the phosphorus dimers. The uptake recorded on the (2×1) by XPS (Fig. 2) is most likely due to adsorption at steps, kinks, and other defect sites. The spectra taken from the samples dosed at elevated temperatures, however, show a strong decrease in the peak intensity, especially the first minimum around 1.8 eV, and to a lesser extent, the positive peak at 3.1 eV.

In Fig. 4, reflectance difference spectra are shown of the $\delta(2\times4)$ reconstruction before and after exposure to 15 000 L O_2 at 300 K. The spectrum of the clean surface exhibits a strong negative peak at 1.85 eV, which is attributed to bonds between first and second layer indium atoms.[34,39] Following oxidation, the spectrum is essentially flat, indicating that the oxygen molecules have inserted into the In–In bonds and eliminated their characteristic valence states. These results illustrate that the indium-rich surface is highly reactive to oxygen at 300 K, while the phosphorus-rich surface is not.

The oxygen uptake on the (2×1) and $\delta(2\times4)$ phases at different temperatures is shown in Fig. 5. A dose of 2.5×10^5 L O_2 was chosen to guarantee that each data point would fall into the ''quasi-saturation'' regime. On the (2×1), the oxygen coverage remains well below a monolayer up to about 400 K. However, above 450 K, the coverage rises exponentially with temperature, achieving a maximum value of 2.2 ML at 620 K. Since phosphorus desorption occurs above 620 K, converting the (2×1) into the (2×4), higher temperatures were not explored for this reconstruction. The oxygen coverage obtained following exposure at 300, 530, and 570 K is in good agreement with the decrease in intensity of the negative peak at 1.8 eV in the RD spectra shown in Fig. 3. On the $\delta(2\times4)$, the oxygen coverage increases from 1.0 ML at 300 K to 5.5 ML at 620 K, and increases only slightly with further heating to 720 K. The slowing of the uptake curve is due to the onset of oxide desorption.[40]

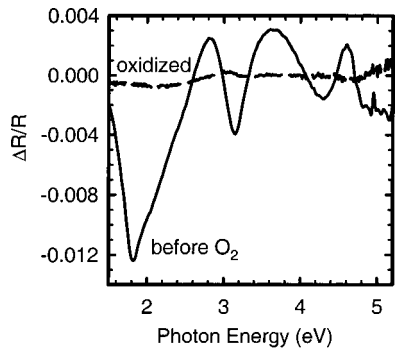

FIG. 4. Reflectance difference spectra of the clean and oxidized $\delta(2\times4)$ surface at 300 K.

Presented in Figure 6 are the P $2p$ and O $1s$ photoemission spectra recorded after oxygen adsorption on the (2×1) surface at different temperatures. The In $3d_{5/2}$ spectra are not shown because they were identical for all the samples, even when recorded at high resolution. This is expected, since the oxygen coverage on the (2×1) is small and the chemical shift of the In $3d_{5/2}$ peak can only be observed when the oxide thickness exceeds several atomic layers.[13] As shown at the bottom of Fig. 6, deconvolution of the O $1s$ line reveals two chemical states of oxygen at 531.4 and 533.2 eV. The intensity ratio of these two features increases from 7:1 to 10:1 as the oxidation temperature is raised from 400 to 620 K. Starting at about 530 K, the phosphorus $2p$ spectrum shows two asymmetric peaks at 128.6 and 133.9 eV, due to the $+3$ and $+5$ valence states of the P atoms, respectively.[41] The saturation uptake of oxygen at 530 K is 0.6 ML.

Figure 7 displays XPS spectra of the $\delta(2\times4)$ reconstruction after oxidation at different sample temperatures. Following O_2 exposure at 300 K, the P $2p$ spectrum exhibits a single band at 128.6 eV, which arises from the phosphorus atoms in bulk indium phosphide. On the other hand, O_2 adsorption at 420 K and above produces a second phosphorus $2p$ peak at 133.9 eV, which is due to P^{+5}. This feature grows in intensity with increasing reaction temperature. The oxygen $1s$ band may be deconvoluted into a main peak at 531.6 eV and two smaller ones at 530.1 and 533.2 eV. The former peak is visible after InP oxidation at 300 to 530 K, while the latter is discernable after InP oxidation at 620 to 720 K. A single indium $3d_{5/2}$ band at 444.3 eV is recorded for oxygen exposures below 620 K. However, at 620 to 720 K, a shoulder at

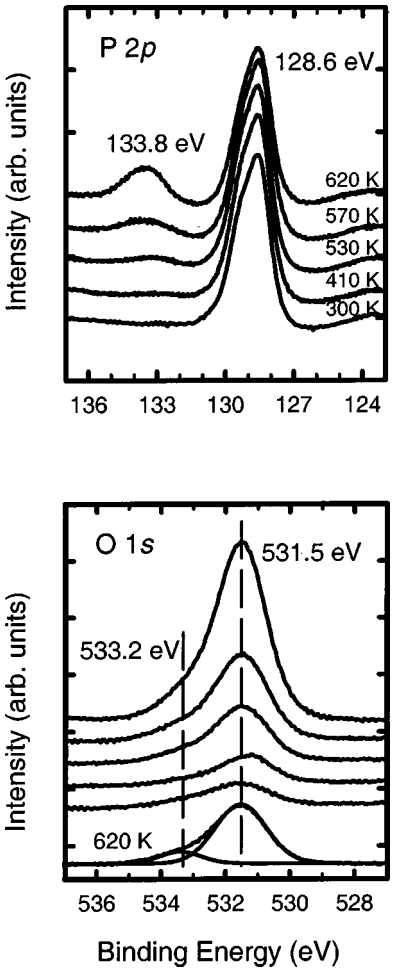

FIG. 6. Phosphorus $2p$ and oxygen $1s$ photoemission spectra of the (2×1) surface after exposure to 2.5×10^5 LO_2 at different temperatures.

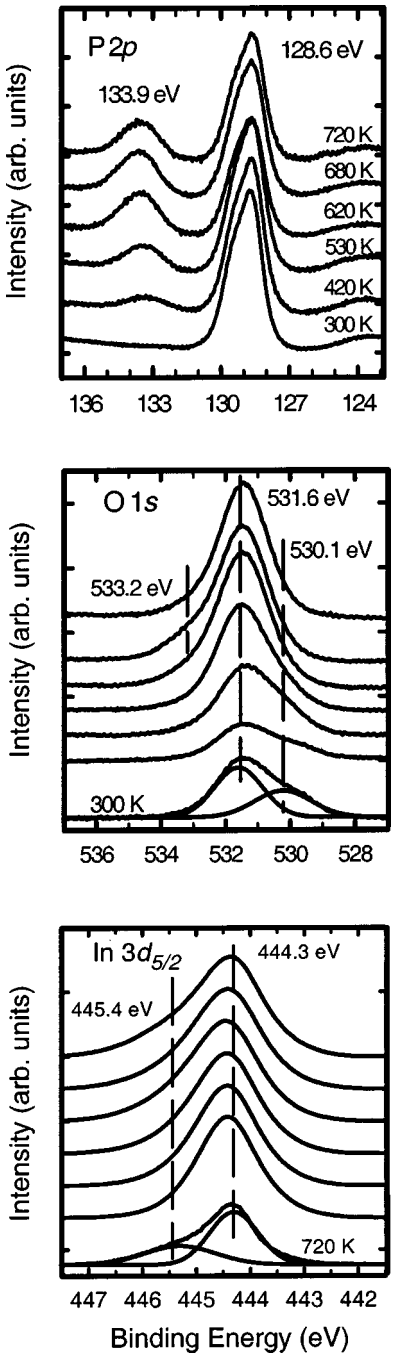

FIG. 7. Phosphorus $2p$, oxygen $1s$, and indium $3d_{5/2}$ photoemission spectra of the $\delta(2\times4)$ surface after exposure to 1.8×10^5 LO_2 at different temperatures.

higher binding energy is detected, which upon deconvolution yields a second small band at 445.4 eV. The deconvoluted In $3d_{5/2}$ spectrum is presented at the bottom of Fig. 7. On InP $\delta(2\times4)$ surfaces dosed with O_2 at 620 to 720 K, the oxygen coverage equals approximately 5.5 ML.

IV. DISCUSSION

The uptake curves in Fig. 2 may be used to estimate the relative rate of oxygen adsorption on the (2×1) and $\delta(2\times4)$ phases. The sticking probability at zero coverage can be estimated as

$$S_0 \approx \frac{\theta_{OX}\cdot N_s}{R_{coll}\cdot \tau}. \tag{3}$$

Here, N_s is the site density (cm^{-2}), R_{coll} is the collision rate of O_2 molecules with the surface (6.8×10^{15} $cm^{-2}\,s^{-1}$ at 300 K and a pressure of 1×10^{-5} Torr), and τ is time (s). The site density is assumed to be 5.8×10^{14} cm^{-2}, which corresponds to the number of (1×1) unit cells in a cm^2 of the InP (001) plane. From Eq. (3) and the initial slopes of the curves in Fig. 2, the sticking probabilities of oxygen on the (2×1) and $\delta(2\times4)$ are estimated to be 1.7×10^{-6} and 1.4×10^{-3}, respectively. The thousand-fold difference in the magnitude of S_0 demonstrates that the reaction of oxygen with the indium phosphide surface is strongly structure sensitive. It should be noted that the oxidation rate calculated above is averaged over all the sites exposed on the surface, including step edges, defects, etc. As the RDS spectra show in Fig. 3, no discernable reaction takes place on the (2×1) terraces at 300 K.

The x-ray photoemission spectra provide information about the nature of the chemical bonds formed between oxygen, indium, and phosphorus on the InP (001) surface. Listed in Table I are the binding energies observed for the In $3d_{5/2}$, P $2p$, and O $1s$ lines in a variety of indium and phosphorous compounds. Indium oxide exhibits In–O–In bonds that yield

TABLE I. Assignment of the XPS binding energies to different chemical states.[a]

Compound	In $3d_{5/2}$	P $2p$	O $1s$
InP	444.4	128.8	
In_2O_3	444.6–444.9		530.2
$InPO_4$	445.7	133.7–134.1	531.8
$In(PO_3)_3$	445.4	133.7	531.5, 533.5
P_2O_5		135.0–135.6	532.7, 533.5

[a]References 26, 40–44.

In $3d_{5/2}$ and O $1s$ binding energies of 444.7 ± 0.2 and 530.2 eV.[42] The In $3d_{5/2}$ line position is only slightly higher than that found in InP. Indium phosphate compounds, $InPO_4$ and $In(PO_3)_3$, produce characteristic In $3d_{5/2}$, P $2p$, and O $1s$ binding energies at 445.5 ± 0.2, 133.9 ± 0.2, and 531.6 ± 0.2 eV, respectively.[26,40–43] These values may be assigned to the In–O–P bonds found in these crystals. The $In(PO_3)_3$ compound exhibits a second O $1s$ line at 533.5 eV that is also observed in P_2O_5.[40,44] This binding energy may be ascribed to P–O–P bonds.

Based on the foregoing discussion, the photoemission results may be used to identify the bond types found in the oxide layers on the two reconstructions. The O $1s$ spectra for the oxidized (2×1) surface (cf., Fig. 6) contain two peaks at 531.4 and 533.2 eV. These binding energies are assigned to the In–O–P and P–O–P bonds. The lower energy band is much more intense than the higher energy one, indicating that most of the bonding in the film is of the In–O–P type. In other words, the oxygen atoms prefer to insert into the In–P back bonds instead of into the phosphorus dimer bonds. This is further supported by the RD spectra presented in Fig. 3. The positive peak at 3.1 eV that is related to the phosphorus dimers does not disappear completely even at an oxygen coverage of approximately 1.0 ML, indicating that some dimers remain unreacted on the surface.

The results obtained for the oxidized $\delta(2\times4)$ surface are a bit more complicated. As shown in Fig. 7, the O $1s$ spectra of samples oxidized at 300 and 410 K contain a main peak at 531.6 eV and a shoulder at 530.1 eV. These features are ascribed to In–O–P and In–O–In bonds, respectively. As the temperature is raised to 720 K, the low binding energy shoulder in the O $1s$ spectrum disappears and is replaced by a high binding energy shoulder at 533.2 eV, due to P–O–P bonds. These results suggest that the oxide layer becomes more phosphorus-rich at high temperature, either due to indium desorption or to phosphorus out-diffusion from the oxide/semiconductor interface.[45,46] The P $2p$ spectra recorded for the $\delta(2\times4)$ show a gradual increase in intensity of the peak at 133.9 eV with increasing oxidation temperature. This corresponds to the growth of the oxide layer on the indium-rich phase. When the temperature exceeds 620 K and the oxygen coverage reaches 5.2 ML, one can finally discern the high binding energy peak at 445.4 eV in the In $3d_{5/2}$ spectrum.

It is well established that molecular oxygen dissociatively chemisorbs onto semiconductor surfaces at 300 K and above.[47,48] In Table II, bond enthalpies related to the chemisorption of O_2 on InP (001) are calculated from the gas-phase diatomic bond energies. Oxygen insertion into In–In, P–P, and In–P bonds is predicted to be an energetically favorable process, with the latter reaction being the most favored on the three. The XPS and RDS data indicate that for both reconstructions the preferred site for oxygen adsorption is the In–P back bond. This same behavior has been observed on Si (100) surfaces, where the oxygen has been found to insert into the Si–Si back bonds.[50–52]

TABLE II. Comparison of In, O, and P bond and reaction enthalpies.[a]

Bonds/Reactions	Enthalpies (kJ/mol)
O–O	498
In–P	198
P–P	490
In–In	100
P–O	600
In–O	320
O_2 + 2 In–In = 2 In–O–In	$\Delta H = -582$
O_2 + 2 P–P = 2 P–O–P	$\Delta H = -919$
O_2 + 2 In–P = 2 In–O–P	$\Delta H = -944$

[a]Reference 49.

The much higher reactivity of oxygen towards the In-rich $\delta(2\times4)$ compared to the P-rich (2×1) can be explained by the difference in dangling bond states on these two reconstructions. On the $\delta(2\times4)$, the indium dangling bonds are empty, so they can initially form a dative bond with the lone pairs on the oxygen molecule. This metastable state can quickly lead to oxygen dissociation and insertion into the In–In and In–P bonds. By contrast, on the (2×1), the phosphorus dangling bonds are either half-filled or filled, thereby blocking electron transfer from the O_2 molecule to the surface.

V. CONCLUSIONS

The oxidation of indium phosphide (001) is an activated process and strongly structure sensitive. On the indium-rich $\delta(2\times4)$ reconstruction, oxygen atoms insert into the In–In dimer and In–P back bonds at room temperature and above, whereas on the phosphorus-rich (2×1) reconstruction, no appreciable adsorption occurs until the sample is heated above 450 K. At these higher temperatures, the O_2 molecules react with both the P–P dimer and In–P back bonds.

ACKNOWLEDGMENT

Funding for this research was provided by the National Science Foundation, Divisions of Chemical and Transport Systems and Materials Research.

[1] M. Losurdo, P. Capezzuto, and G. Bruno, Phys. Rev. B **56**, 10621 (1997).
[2] W. Liu, *Fundamental of III-V Devices* (Wiley, New York, 1999).
[3] S. Yngvesson, *Microwave Semiconductor Devices* (Kluwer, Boston, 1991).
[4] J. Müllrich *et al.*, IEEE J. Solid-State Circuits **35**, 1260 (2000).
[5] D. Yap, K. R. Elliott, Y. K. Brown, A. R. Kost, and E. S. Ponti, IEEE Photonics Technol. Lett. **13**, 626 (2001).
[6] M. T. Camargo Silva, J. E. Zucker, L. R. Carrion, C. H. Joyner, and A. G. Dentai, IEEE J. Sel. Top. Quantum Electron. **6**, 26 (2000).
[7] K. W. Kobayashi *et al.*, IEEE Microwave Guid. Wave Lett. **7**, 353 (1997).
[8] V. Devnath, K. N. Bhat, and P. R. S. Rao, IEEE Electron Device Lett. **18**, 114 (1997).

[9] R. Driad, W. R. McKinnon, Z. H. Lu, and S. P. McAlister, J. Electron. Mater. **29**, L33 (2000).
[10] G. Hollinger, E. Bergignat, J. Joseph, and Y. Robach, J. Vac. Sci. Technol. A **3**, 2082 (1985).
[11] I. K. Han, E. K. Kim, J. I. Lee, S. H. Kim, K. N. Kang, Y. Kim, H. Lim, and H. L. Park, J. Appl. Phys. **81**, 6986 (1997).
[12] Y. Robach, M. P. Besland, J. Joseph, G. Hollinger, P. Viktorovitch, P. Ferret, M. Pitaval, A. Falcou, and G. Post, J. Appl. Phys. **71**, 2981 (1997).
[13] A. Nelson, K. Geib, and C. W. Wilmsen, J. Appl. Phys. **54**, 4134 (1983).
[14] Y. Chen, J. M. Seo, S. G. Anderson, and J. H. Weaver, Phys. Rev. B **44**, 1699 (1991).
[15] A. Funyu, S. Sato, and H. Ikoma, Jpn. J. Appl. Phys., Part 2 **34**, L968 (1995).
[16] C. W. Wilmsen, R. W. Kee, and K. M. Geib, J. Vac. Sci. Technol. **16**, 1434 (1979).
[17] F. Schroder, W. Storm, M. Altebockwinkel, L. Wiedmann, and A. Benninghoven, J. Vac. Sci. Technol. B **10**, 1291 (1992).
[18] P. Schmuki, G. I. Sproudle, J. A. Bardwell, Z. H. Lu, and M. J. Graham, J. Appl. Phys. **79**, 7303 (1996).
[19] T. Block (TRW, private communication).
[20] A. Huelsman, Compound Semicond. **7**, 7 (2001).
[21] H. Takeuchi *et al.*, IEEE J. Sel. Top. Quantum Electron. **3**, 336 (1997).
[22] D. Huber *et al.*, J. Lightwave Technol. **18**, 992 (2000).
[23] G. Rondeau, S. Biblemont, J. Decobert, and G. Post, *Proceedings of the 2000 International Conference on Indium Phosphide and Related Materials* (IEEE, Piscataway, NJ, 2000), p. 333.
[24] I. Deyhimy, Compound Semicond. **7**, 77 (2001).
[25] E. A. Irene, Mater. Sci. Forum **185–188**, 37 (1995).
[26] S. J. Hoekje and G. B. Hoflund, Thin Solid Films **197**, 367 (1991).
[27] X. Liu, J. W. Andrews, and E. A. Irene, J. Electrochem. Soc. **138**, 1106 (1995).
[28] M. Losurdo, P. Capezzuto, and G. Bruno, J. Vac. Sci. Technol. B **14**, 691 (1996).
[29] L. Li, B.-K. Han, Q. Fu, and R. F. Hicks, Phys. Rev. Lett. **82**, 1879 (1999).
[30] M. J. Begarney, L. Li, C. H. Li, D. C. Law, Q. Fu, and R. F. Hicks, Phys. Rev. B **62**, 8092 (2000).
[31] L. Li, Q. Fu, C. H. Li, B.-K. Han, and R. F. Hicks, Phys. Rev. B **61**, 10223 (2000).
[32] M. J. Begarney, C. H. Li, D. C. Law, S. B. Visbeck, Y. Sun, and R. F. Hicks, Appl. Phys. Lett. **78**, 55 (2001).
[33] P. Vogt, T. Hannappel, S. Visbeck, K. Knorr, N. Esser, and W. Richter, Phys. Rev. B **60**, R5117 (1999).
[34] W. G. Schmidt, N. Esser, A. M. Frisch, P. Vogt, J. Bernholc, F. Bechstedt, M. Zorn, T. Hannappel, S. B. Visbeck, F. Willig, and W. Richter, Phys. Rev. B **61**, R16335 (2000).
[35] L. Li, B.-K. Han, D. Law, C. H. Li, Q. Fu, and R. F. Hicks, Appl. Phys. Lett. **75**, 683 (1999).
[36] Y. Feurprier, Ch. Cardinaud, and G. Turban, J. Vac. Sci. Technol. B **16**, 1823 (1998).
[37] Z. H. Lu, B. Bryshiewicz, J. McCaffrey, Z. Wasilewski, and M. J. Graham, J. Vac. Sci. Technol. B **11**, 2033 (1993).
[38] T. Hannappel, S. Visbeck, M. Zorn, J.-T. Zettler, and F. Willig, J. Cryst. Growth **221**, 124 (2000).
[39] D. C. Law, Q. Fu, S. B. Visbeck, Y. Sun, C. H. Li, and R. F. Hicks, Surf. Sci. **496**, 121 (2002).
[40] P. Streubel, H. Peisert, R. Hesse, T. Chasse, and R. Szargan, Surf. Interface Anal. **23**, 581 (1999).
[41] C. D. Wagner, W. M. Riggs, L. E. Davis, J. F. Moulder, and G. E. Muilenberg, *Handbook of X-Ray Photoelectron Spectroscopy* (Perkin-Elmer, Eden Prairie, MN, 1979).
[42] J. T. Wolan and G. B. Hoflund, J. Vac. Sci. Technol. A **16**, 2546 (1998).
[43] G. Hollinger, J. Joseph, Y. Robach, E. Bergignat, B. Commère, P. Viktorovitch, and M. Froment, J. Vac. Sci. Technol. B **5**, 1108 (1987).
[44] G. D. Khattak, M. A. Salim, A. S. Al-Harthi, D. J. Thompson, and L. E. Wenger, J. Non-Cryst. Solids **212**, 180 (1997).
[45] R. F. C. Farrow, J. Phys. D **7**, 2436 (1974).
[46] Ph. Ebert, M. Heinrich, M. Simon, K. Urban, and M. G. Lagally, Phys. Rev. B **51**, 9696 (1995).
[47] W. Mönch, *Semiconductor Surfaces and Interfaces* (Springer-Verlag, Berlin, 1993).
[48] D. J. Frankel, J. R. Anderson, and G. J. Lapeyre, J. Vac. Sci. Technol. B **1**, 763 (1983).
[49] *CRC Handbook of Chemistry and Physics 1999–2000: A Ready-Reference Book of Chemical and Physical Data*, 81st ed., edited by D. R. Lide (CRC Press, Boca Raton, FL, 2000).
[50] B. B. Stefanov, A. B. Gurevich, M. K. Weldon, K. Raghavachari, and Y. J. Chabal, Phys. Rev. Lett. **81**, 3908 (1998).
[51] M. K. Weldon, B. B. Stefanov, K. Raghavachari, and Y. J. Chabal, Phys. Rev. Lett. **79**, 2851 (1997).
[52] K. Kato, T. Uda, and K. Terakura, Phys. Rev. Lett. **80**, 2000 (1998).